

## The ROSAT bright source 1RXS J201607.0+251645: an active Algol-type binary \*

Hua-Li Li<sup>1,2,3</sup>, Yuan-Gui Yang<sup>1,4</sup>, Wei Su<sup>1,3</sup>, Hui-Juan Wang<sup>1,3</sup> and Jian-Yan Wei<sup>1</sup>

<sup>1</sup> National Astronomical Observatories, Chinese Academy of Sciences, Beijing 100012, China;  
*lhl@bao.ac.cn*

<sup>2</sup> National Astronomical Observatories / Urumqi Observatory, Chinese Academy of Sciences, Urumqi 830011, China

<sup>3</sup> Graduate University of Chinese Academy of Sciences, Beijing 100049, China;

<sup>4</sup> School of Physics and Electric Information, Huaibei Coal Industry Teachers College, Huaibei 235000, China

Received 2009 March 25; accepted 2009 May 18

**Abstract** 1RXS J201607.0+251645 is identified as an eclipsing binary. We present preliminary observations in the *V* band with the 0.6-m telescope for three years and extensive observations in the *V* and *R* bands with the 0.8-m telescope for six nights, respectively. The light curve of the system is *EB* type. Five light minimum times were obtained and the orbital period of  $0.388058^d (\pm 0.00044^d)$  is determined. The photometric solution given by the 2003-version of the Wilson-Devinney program suggests that the binary is a semi-detached system with photometric mass ratio  $0.895 (\pm 0.006)$ , which is probably comprised of a G5 primary and an oversized K5 secondary. The less massive component has completely filled its Roche lobe, while the other one almost fills its Roche lobe with a filling factor of 93.4%. The system shows a varying O'Connell effect in its phase folded diagrams from 2005 to 2007, and is X-ray luminous with  $\log L_X/L_{bol} \sim -3.27$ . Possible mechanisms to account for these two phenomena are discussed. Finally, we infer that the binary may be in thermal oscillation or may evolve into a contact binary.

**Key words:** stars: binaries: close — stars: binaries: eclipsing — stars: individual: 1RXS J201607.0+251645, HD 339946

### 1 INTRODUCTION

Algol type binaries are eclipsing variables with the less massive component filling its Roche lobe and transferring material to its companion (Ziolkowski 1969; Proper 1989). They are X-ray emitters (Shaw & Cailiault 1996), similar to solar analogs such as RS CVn binaries (Umana et al. 1991). The driving mechanisms of X-ray emission in these systems remain unsolved though they are generally thought to be related to large scale mass transfer (Sarna et al. 1998), chromospheric activity in the components (Hall 1989; Retter et al. 2005), or hot disk activity (Blondin et al. 1995). Finding more of them may help to shed light on their X-ray nature.

The optical variability campaign for strong X-ray sources with the 0.6-m telescope at the Xinglong Observatory was launched in 2005, aiming to study long term chromospheric activity of young stars.

\* Supported by the National Natural Science Foundation of China.

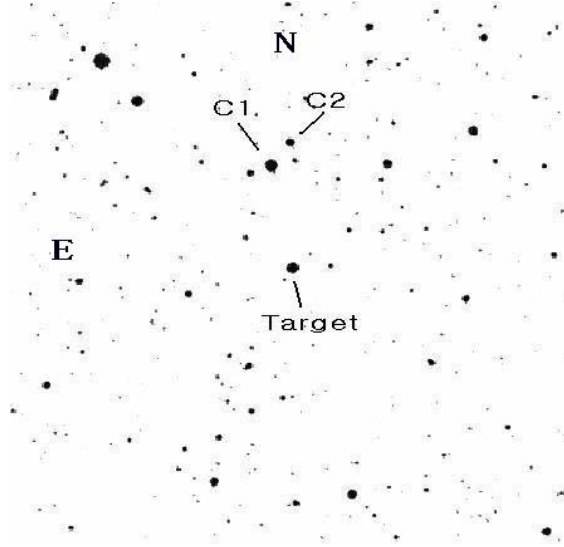


**Fig. 1** Chart of findings from 1RXS J201607.0+251645 made from a  $V$  band CCD image taken by the 0.8-m telescope. The field of view is  $11' \times 11'$ . C1 and C2 are used as the comparison and check stars, respectively.

Containing about 200 objects (many of which have never been identified) in the sample selected from the ROSAT bright source catalog (RBS) (Voges et al. 1999), the campaign is an excellent resource for finding new variables. 1RXS J201607.0+251645 ( $\alpha_{2000.0} = 20^{\text{h}}16^{\text{m}}07.0^{\text{s}}$ ,  $\delta_{2000.0} = 25^{\circ}16'45.0''$ ) was included in our observing program and piqued our interest by its obvious eclipsing nature.

The  $1\sigma$  positional error for 1RXS J201607.0+251645 is  $9''$ , including  $8''$  of systematic error. Within this error circle, we found a bright star HD 339946 (also known as GSC 02159–01213, TYC 2159–1213–1, and 2MASS J20160698+2516536) lying  $8.8''$  from the X-ray position. Thus, HD 339946 is taken as the optical counterpart of 1RXS J201607.0+251645. It is listed in SIMBAD as a G5 star, with a  $V$  band magnitude of  $10.6^{\text{m}}$ . No previous description of variability could be found in the General Catalog of Variable Stars (GCVS) (Kholopov et al. 1998) or other literature.

## 2 OBSERVATIONS AND PHASE CALCULATIONS

Our first set of photometric observations of 1RXS J201607.0+251645 was performed with the 0.6-m telescope at the Xinglong Observatory from 2005 November to 2007 September. Typical observing frequency was several times per night using auto-observation mode. A PI  $1024 \times 1024$  CCD and Standard Johnson  $V$  filter were used. The field of view was  $17' \times 17'$  (Xing et al. 2006).

Preliminary analysis had revealed the eclipsing effect of the target. In order to investigate its eclipsing nature in more detail, extensive observations were conducted in 2008 November with the 0.8-m Tsinghua-NAOC telescope (TNT) at the Xinglong Observatory. TNT employs a PI  $1340 \times 1300$  CCD, giving a field of view of  $11' \times 11'$  (Zheng et al. 2008). Standard Johnson  $V$  band and  $R$  band light curves were obtained. A chart of the findings made from a  $V$ -band CCD image taken by the 0.8-m telescope is shown in Figure 1, with the comparison star and check star marked as C1 and C2 (Table 1), respectively.

All photometric reductions were performed with IRAF<sup>1</sup> including bias and dark subtraction and flat-field correction. No differential extinction was applied since the angular distances of all the stars

---

<sup>1</sup> IRAF is distributed by the National Optical Astronomy Observatory, which is operated by the Association of Universities for Research in Astronomy, Inc., under a cooperative agreement with the National Science Foundation.

**Table 1** Details of Target Star, Comparison Star and Check Star in Our Observation

Star	$\alpha_{2000.0}$	$\delta_{2000.0}$	mag ( $V$ )
Target	20:16:06.98	25:16:53.8	10.6 <sup>m</sup>
C1	20:16:20.02	25:20:13.7	10.3 <sup>m</sup>
C2	20:16:06.90	25:19:21.8	11.0 <sup>m</sup>

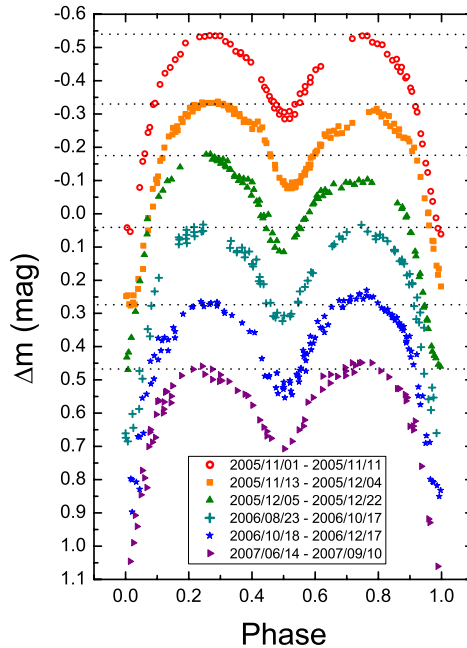


**Fig. 2** Phase folded diagrams of 1RXS J201607.0+251645 from 2005 to 2007, which were made with the data obtained in the 0.6-m telescope. They are arbitrarily shifted for display purposes.

were small. The resulting photometric accuracy is estimated to be 0.01<sup>m</sup> for observations with the 0.6-m telescope and 0.005<sup>m</sup> for those with the 0.8-m telescope.

For preliminary observations, phase folded diagrams in Figure 2 were plotted with a period of 0.388<sup>d</sup> obtained with the phase dispersion minimization (PDM) method (Stellingwerf 1978).

In 2008, we obtained 648 and 645 extensive observations in the  $V$  and  $R$  bands, which are shown in Figure 3 and listed in Appendix A. The light curves vary continuously between eclipses, indicating that the system is an *EB* type eclipsing binary (Sterken et al. 2005). The amplitudes of various light curves are 0.52<sup>m</sup> and 0.51<sup>m</sup> in the  $V$  and  $R$  bands, respectively. The primary eclipse is deeper than the secondary eclipse by up to 0.32<sup>m</sup> in the  $V$  band and 0.29<sup>m</sup> in the  $R$  band.

Five light minimum times were obtained in the extensive observations (Table 2). Using the linear least-squares method, the ephemeris formula could be given as follows:

$$\text{Min. I.} = \text{HJD}2454771.6336(\pm 0.0037) + 0.388058(\pm 0.00044) \times E. \quad (1)$$

### 3 PHOTOMETRIC SOLUTION

The photometric solution was calculated with the 2003 version of the Wilson-Devinney program (Wilson & Devinney 1971; Wilson 1990, 1994). Before running the differential corrections (DC) pro-

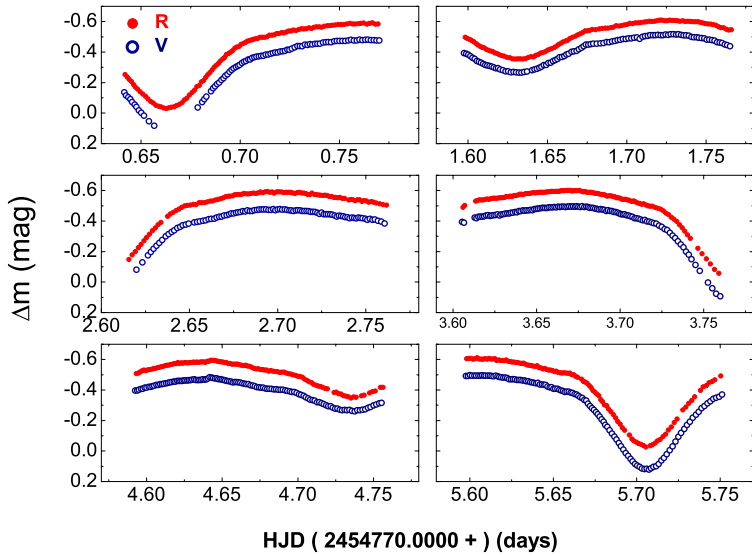


**Fig. 3**  $V, R$ -band light curves of 1RXS J201607.0+251645 covering 6 nights with the 0.8-m telescope.

**Table 2** Light Minimum Times of 1RXS J201607.0+251645

HJD	Band	Error
2454770.6629	$R$	0.0001
2454771.6314	$VR$	0.0002
2454774.7470	$VR$	0.0003
2454775.7047	$VR$	0.0007
2454776.6755	$R$	0.0004

gram, a series of input parameters were fitted. The temperature of the primary component was initially set at 5160 K (Cox 2000), in accordance with the G5 dwarf spectral type given in SIMBAD (operated at CDS). The gravity-darkening coefficients  $g_1$  and  $g_2$  were set at the same value of 0.32 (Lucy 1967), assuming convective atmospheres of the two components. The bolometric albedos were fixed at  $A_1 = A_2 = 0.5$  (Rucinski 1973). Linear limb-darkening coefficients for Star 1 were  $x_{1V} = 0.65$  and  $x_{1R} = 0.51$ , respectively (Al-Naimiy 1978). Meanwhile, the limb-darkening coefficients for Star 2 (i.e.,  $x_{2V}$  and  $x_{2R}$ ) were determined according to its temperature  $T_2$ . Based on the temperatures, convective atmospheres were assumed. The commonly adjustable parameters employed are the orbital inclination  $i$ , the mass ratio  $q$ , the mean temperature of Star 2  $2T_2$ , the potential of the components  $\Omega_1$ , and the monochromatic luminosity of Star 1  $L_1$ . The reflection effect was computed with the detailed model of Wilson (1990). The relative brightness of Star 2 was calculated by the stellar atmosphere model.

To find a photometric mass ratio, solutions were obtained for a series of trial values of the mass ratio ( $q = 0.2 - 2.0$ ). For each value of the mass ratio, the calculation started at mode 2 (i.e., detached mode), but the solution always converged to mode 5 (i.e., semi-detached mode), suggesting that the secondary has completely filled its Roche lobe. Corresponding mass ratios and squared residuals are plotted in Figure 4, where the smallest value of  $\Sigma(O - C)_i^2$  is located at  $q \sim 0.8$ . At this point, the set of adjustable parameters was expanded to include the mass ratio  $q$ . After a few trials and corrections of the mass ratio, a best-fit solution was achieved at  $q = 0.895(\pm 0.006)$ . The photometric elements are

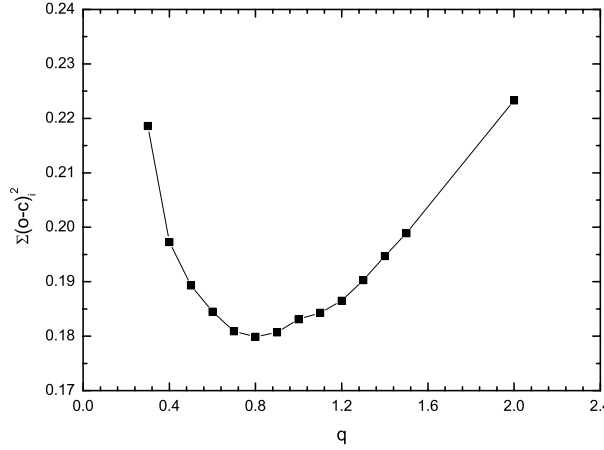


**Fig. 4** The relation of  $\sum -q$  for 1RXS J201607.0+251645.

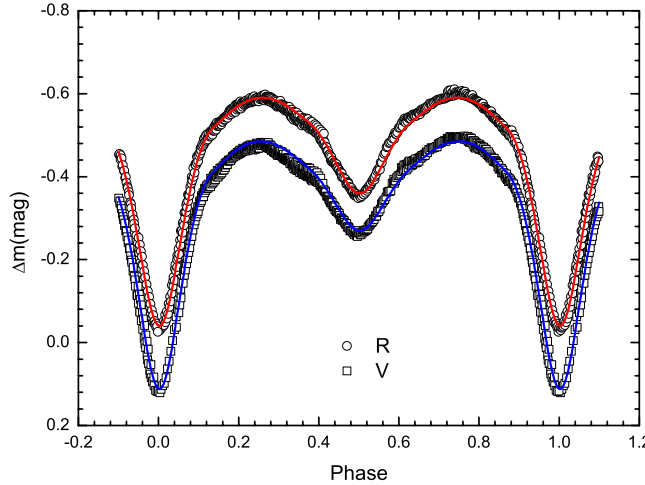


**Fig. 5** Light curves of 1RXS J201607.0+251645. The open circles and squares represent *V* and *R* observations. The lines were calculated from the photometric solution.

listed in Table 3. Synthesis light curves as solid lines are plotted in Figure 5, where the quality of the fits is fairly good in the *V* and *R* bands.

## 4 DISCUSSIONS

### 4.1 Optical Variability Outside of the Eclipse

As shown in Figure 2, earlier observations had revealed the existence of the O'Connell effect (Milone 1968) in 1RXS J201607.0+251645, which was varying along with time. To carefully examine how this asymmetry varied, we plot the primary maximum brightness (Max. I, in magnitude), the secondary maximum brightness (Max. II, in magnitude) and the values of Max. II – Max. I of each phase folded diagram, as shown in Figure 6. Clearly, the O'Connell effect was varying dramatically at the end of

**Table 3** Light-curve Solution for 1RXS J201607.0+251645

Parameters	Values
$i(^{\circ})$	70.16( $\pm 0.06$ )
$q = M_2/M_1$	0.895( $\pm 0.006$ )
$T_1(K)$	5560
$T_2(K)$	4301( $\pm 8$ )
$\Omega_1$	3.7364( $\pm 0.0118$ )
$\Omega_2 = \Omega_{\text{in}}$	3.5856
$L_1/(L_1 + L_2)_V$	0.8298( $\pm 0.0070$ )
$L_1/(L_1 + L_2)_R$	0.7717( $\pm 0.0056$ )
$x_{2V}$	0.85
$x_{2R}$	0.68
$r_1$ (pole)	0.3454( $\pm 0.0015$ )
$r_1$ (side)	0.3602( $\pm 0.0018$ )
$r_1$ (back)	0.3826( $\pm 0.0024$ )
$r_1$ (point)	0.4116( $\pm 0.0041$ )
$r_2$ (pole)	0.3465( $\pm 0.0005$ )
$r_2$ (side)	0.3635( $\pm 0.0006$ )
$r_2$ (back)	0.3948( $\pm 0.0006$ )
$r_2$ (point)	0.4881( $\pm 0.0022$ )
$\sum(O - C)_i^2$	0.1828

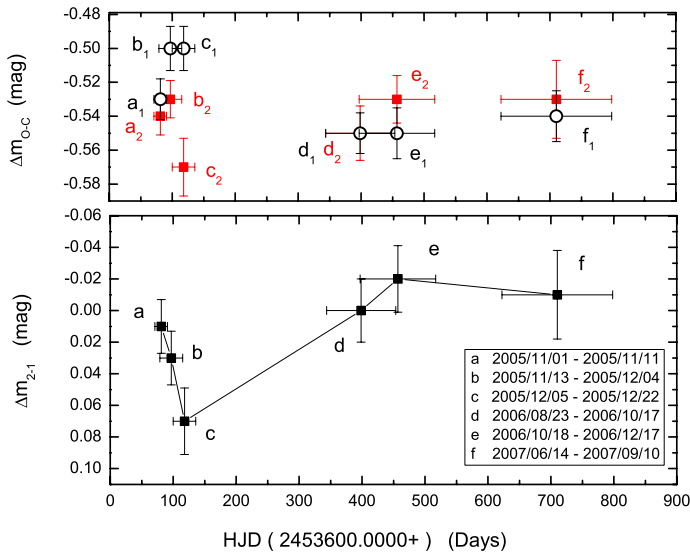


**Fig. 6** Top: maximum brightness VS. HJD. Subscripts “1” and “2” denote the primary maximum brightness (Max. I, in magnitude) and the secondary maximum brightness (Max. II, in magnitude). Bottom: Max. II–Max. I versus HJD.

2005: Max. I brightened by about 0.03<sup>m</sup> in 2005 November and Max. II darkened by about 0.04<sup>m</sup> in 2005 December. Since 2006, the change of asymmetry was mild.

The varying O’Connell effect is also reported in other active binaries, such as GR Tauri (Gu et al. 2004), U Pegasi (Djurasevic 2001), XY UMa (Pribulla et al. 2001) and EQ Tau (Yuan & Qian 2007), in which the varying O’Connell effect is usually modeled and explained by the development and migration of hot spots (Gu et al. 2004) or dark spots (Yuan & Qian 2007; Djurasevic 2001; Pribulla et al. 2001).

Because of this, we suggest that either chromospheric activity (Strassmeier et al. 1989; Strassmeier & Bopp 1992; Strassmeier et al. 2008) or the impact of transferred mass streams onto the primary star (Pereira et al. 2006; Ibanoglu et al. 2006) is very strong in our target. Also, the actual situation is likely to be a combination of both processes.

#### 4.2 The X-ray Emission

Based on the conversion relation given by Schmitt et al. (1995):

$$\text{flux} = (5.3 \times \text{HR1} + 8.31) \times 10^{-12} \times \text{counts s}^{-1} [\text{erg cm}^{-2} \text{s}^{-1}] \quad (2)$$

the ROSAT count-rate of  $0.111 \pm 0.016 \text{ c s}^{-1}$  and hardness ratio  $\text{HR1}=0.07 \pm 0.13$  of 1RXS J201607.0+251645 yields a 0.1–2.4 keV flux of  $9.6 \times 10^{-12} \text{ erg cm}^2 \text{s}^{-1}$ . Its distance is  $19.9^{+292.6}_{-9.6} \text{ pc}$ , corresponding to a parallax  $\pi = 50.30 \pm 47.10 \text{ mas}$  (ESA 1997). Hence,  $\log L_X = 28.7^{+2.4}_{-0.6} \text{ erg s}^{-1}$ . Combining its apparent magnitude of  $10.6^m$ , we derived  $\log L_X/L_{\text{bol}} \sim -3.27$ .

Since the source is located outside of a nearby molecular cloud, interstellar absorption should be marginal. As for the internal absorption, it is hard to estimate (Feigelson et al. 2002; Stassun et al. 2004).

Our calculated  $\log L_X$  is a little lower compared to the statistical values of near-contact binaries made by Shaw et al. (1996), while  $\log L_X$  is in the range of 29.09 to 30.55  $\text{erg s}^{-1}$ . However, it is still consistent with their study if we take the large uncertainty of distance into account. In fact, the value of  $\log L_X/L_{\text{bol}}$  is more reliable since it is independent of distance. It falls in the high end of the statistical range of  $-3.2$  to  $-4.1$ , suggesting that the binary is X-ray luminous.

The X-ray emission in the Algol systems are generally considered to originate from chromospheric activity, interacting material, a hot ( $> 10^6 \text{ K}$ ) disk (Richards & Albright 1993; Retter et al. 2005) or an extended “halo” that pervades the entire system (Siarkowski et al. 1996). Chromospheric activity is the most probable mechanism for our target. Since both components of our target are cool stars with effective temperatures lower than that of the Sun, the surfaces on the two components should show deep convective activity. It is generally believed that convective motions generate acoustic and MHD waves that propagate upward and heat the chromosphere and corona (Sarna et al. 1998), which can account for the strong X-ray emission in this system. If true, its variability outside the eclipse could be easily understood, because a strongly convective envelope of cool stars can also account for a comparative amount of dark spots. Besides, the X-ray emission might also be attributed to the interaction between the infalling stream and the star (Sarna et al. 1998) or the extended “halo” that pervades the entire system (Siarkowski et al. 1996). We do not exclude these possibilities in our target, because of the near-contact configuration of the system, as discussed in a later section. For the mechanism of a hot disk, spectral observation is needed to identify its existence or absence.

#### 4.3 The Evolutionary Status

The photometric solution suggests that 1RXS J201607.0+251645 is a semi-detached binary, with the less massive component already filling its Roche lobe. For the primary, the size of its Roche lobe can be determined according to the formula (Eggleton 1983)

$$R_L^i = \frac{0.49(m_i/m_j)^{\frac{2}{3}}}{0.6(m_i/m_j)^{\frac{2}{3}} + \ln [1 + (m_i/m_j)^{\frac{1}{3}}]} \cdot \quad (3)$$

The fill-out factor is defined as  $f = r/R$  (Zhai et al. 1989), where  $r$  denotes the mean relative radius. With the above two relations, the filling factor of the primary is calculated to be 93.4%. This implies that the primary star is very close to completely filling its Roche lobe. Therefore, we may infer that the two components of 1RXS J201607.0+251645 are in near-contact (Shaw 1994). The 3D description of the system given by the light and velocity curve (LC) algorithm of the Wilson-Devinney program is shown in Figure 7.

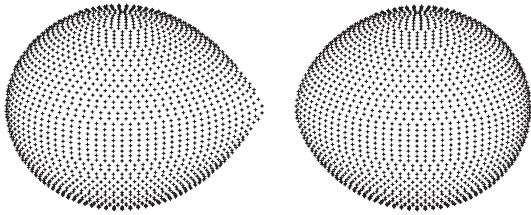


**Fig. 7** 3D representation for 1RXS J201607.0+251645 at phase 0.75.

Suppose the primary is a main-sequence star and its mass and radius could be given as  $M_1 = 0.92M_\odot$  and  $R_1 = 0.92R_\odot$  (Cox 2000) according to its spectral type G5. The secondary component should be a K5 type star according to its temperature given by the photometric solution. Meanwhile, with mass ratio and radius ratio, we could derive the absolute parameters of the secondary as  $M_2 = 0.82M_\odot$  and  $R_2 = 0.98R_\odot$ . This calculation gives an oversized configuration to the secondary component.

Statistics show that semi-detached short-period ( $P < 5$  d) Algols should lose significant amounts of angular momenta (Ibanoglu et al. 2006). If angular momentum loss is continuing in this binary, we could expect that its orbital period is decreasing (Yang & Wei 2009). With the on-going mass transfer, 1RXS J201607.0+251645 may be in thermal oscillation predicted by thermal relaxation oscillation theory (Lucy & Wilson 1979). Another possibility is that it will completely fill its primary component and finally evolve into a contact binary (Bradstreet & Guinan 1994).

## 5 CONCLUSIONS

1RXS J201607.0+251645 is identified to be an *EB* type eclipsing binary based on the morphology of its light curve. The photometric result reveals that it is a semi-contact Algol type system with the less massive component completely filling its Roche lobe. The photometric mass ratio and orbital period are  $0.895(\pm 0.006)$  and  $0.38805^d$ , respectively. Optical variability outside the eclipse of this system showed a varying O'Connell effect in its phase folded light diagrams, which is likely due to hot spots generated by accretion or dark spots from chromospheric activity. The system is X-ray luminous with  $\log L_X/L_{\text{bol}} \sim -3.27$ . The actual process that accounts for its X-ray emission is not yet clear, nevertheless, possible mechanisms are discussed. The system is likely to be comprised of a G5 primary and an oversized K5 secondary. It may be in thermal oscillation or may evolve into a contact binary.

**Acknowledgements** We wish to thank the referee for suggesting a number of improvements to this paper. We are indebted to Drs. Yu-Lei Qiu and Li Cao for providing the original version of the reduction programs. Also, we are grateful to night assistants and the technical support staff for their assistance during the observations, as well as to the astronomers at the Xinglong Observatory, especially Prof. Jing-Yao Hu, Drs. Xiao-Jun Jiang, Jing-Song Deng and Jing Wang for helpful discussion, and to Wei-Kang Zheng, Xu-Hui Han and Li-Ping Xin for catching errors in our manuscript. This work was supported by the National Natural Science Foundation of China (Grant Nos. 10778707 and 10473013). We have made use of the ROSAT data Archive of the Max-Planck-Institut für extraterrestrische Physik at Garching, Germany, as well as the SIMBAD database, operated at CDS, Strasbourg, France.

## References

- Al-Naimiy, H. M. 1978, *Ap&SS*, 53, 181  
 Blondin, J. M., Richards, M. T., & Malinowski, M. L. 1995, *ApJ*, 445, 939  
 Bradstreet, D. H., & Guinan, E. F. 1994, *ASPC*, 56, 228  
 Cox, A. N. 2000, *Allen's Astrophysical Quantities* (4th ed.; New York: Springer)  
 Djurasevic, G. 2001, *A&A*, 367, 840  
 Eggleton, P. P. 1983, *ApJ*, 268, 368  
 ESA 1997, *The Hipparcos and Tycho Catalogues* European Space Agency SP-1200 (Noordwijk:ESA)  
 Feigelson, E. D., Broos, P., Gaffney, J. A. III, et al. 2002, *ApJ*, 574, 258  
 Gu, S. H., Chen, P. S., Choy, Y. K., et al. 2004, *A&A*, 423, 607  
 Hall, D. S. 1989, *Space Sci. Rev.*, 50, 219  
 Ibanoglu, C., Soydugan, F., Soydugan, E., & Dervisoglu, A. 2006, *MNRAS*, 373, 435  
 Khlopov, P. N., et al. 1998, in *Combined General Catalogue of Variable stars*, 4.1 Ed (II/214A)  
 Lucy, L. B. *ApJ*, 205, 208  
 Lucy, L. B., & Wilson, R. E. 1979, *ApJ*, 231, 502  
 Milone, E. E. 1968, *AJ*, 73, 708  
 Pereira, P. C. R., Santos-Junior, J. M., Pilling, D. A., et al. 2006, *Peremennye Zvezdy*, 26, 6  
 Pribulla, T., Chochoł, D., Heckert, P. A., et al. 2001, *A&A*, 371, 997  
 Proper, D. 1989, *ApJS*, 71, 595  
 Retter, A., Richards, M. T., & Wu, K. 2005, *ApJ*, 621, 417  
 Richards, M. T., & Albright, G. E. 1993, *ApJ*, 88, 199  
 Rucinski, S. M. 1973, *Acta Astronomica*, 23, 79  
 Sarna, M. J., Yerli, S. K., & Muslimov, A. G. 1998, *MNRAS*, 297, 760  
 Schmitt, J. H. M. M., Fleming, T. A., & Giampapa, M. S. 1995, *ApJ*, 450, 392  
 Shaw, J. S. 1994, *Mem. Soc. Astron. Ital.*, 65, 95  
 Shaw, J. S., Cailiault, J. P., & Schmitt, J. H. M. M. 1996, *ApJ*, 461, 951  
 Siarkowski, M., Pres, P., Darke, S. A., et al. 1996, *ApJ*, 473, 470  
 Stassun, K. G., Ardila, D. R., Barsony, M., et al. 2004, *AJ*, 127, 3537  
 Stellingwerf, R. F. 1978, *ApJ*, 224, 953  
 Strassmeier, K. G., Hall, D. S., Boyd, L. J., et al. 1989, *AJ*, 69, 141  
 Strassmeier, K. G., & Bopp, B. W. 1992, *A&A*, 259, 183  
 Strassmeier, K. G., Briguglio, R., Granzer, T., et al. 2008, *A&A*, 490, 287  
 Sterken, C., & Jaschek, C. 2005, *Light Curves of Variable Stars*, (Cambridge: Cambridge University Press)  
 Umana, G., Catalano, S., & Rodono, M. 1991, *A&A*, 249, 217  
 Voges, W., Aschenbach, B., Boller, T., et al. 1999, *A & A*, 349, 389  
 Wilson, R. E. 1990, *ApJ*, 356, 613  
 Wilson, R. E. 1994, *PASP*, 106 921  
 Wilson, R. E., & Devinney, E. J. 1971, *ApJ*, 166, 605  
 Xing, L. F., Zhang, X. B., & Wei, J. Y. 2006, *ChJAA* (*Chin. J. Astron. Astrophys.*), 6, 716  
 Yang, Y. G., & Wei, J. Y. 2009, *AJ*, 137, 226  
 Yuan, J. Z., & Qian, S. B. 2007, *MNRAS*, 381, 602  
 Zhai, D. S., Zhang, X. Y., & Zhang, R. X. 1989, *Acta Astron. Sinica*, 30, 225  
 Zheng, W. K., Deng, J. S., Zhai, M., et al. 2008, *ChJAA* (*Chin. J. Astron. Astrophys.*), 8, 693  
 Ziolkowski, J. 1969, *Ap&SS*, 3, 14

## Appendix A:

**Table A.1** *V* Band Observations of 1RXS J201607.0+251645

HJD +2454770	$\Delta$ (m)								
0.6415	-0.136	0.6425	-0.116	0.6436	-0.104	0.6446	-0.091	0.6456	-0.072
0.6467	-0.057	0.6477	-0.041	0.6489	-0.018	0.6501	-0.003	0.6514	0.016
0.6540	0.053	0.6567	0.083	0.6786	-0.037	0.6808	-0.072	0.6819	-0.091
0.6830	-0.108	0.6852	-0.143	0.6863	-0.162	0.6873	-0.175	0.6884	-0.19
0.6894	-0.202	0.6905	-0.217	0.6915	-0.229	0.6925	-0.245	0.6936	-0.256
0.6946	-0.271	0.6957	-0.284	0.6967	-0.293	0.6977	-0.303	0.6988	-0.31
0.6998	-0.316	0.7008	-0.329	0.7019	-0.338	0.7029	-0.342	0.7040	-0.351
0.7050	-0.352	0.7060	-0.361	0.7071	-0.367	0.7082	-0.371	0.7094	-0.372
0.7105	-0.376	0.7117	-0.376	0.7129	-0.382	0.7141	-0.385	0.7153	-0.389
0.7165	-0.393	0.7177	-0.399	0.7189	-0.399	0.7201	-0.404	0.7213	-0.406
0.7225	-0.409	0.7237	-0.416	0.7248	-0.416	0.7260	-0.422	0.7275	-0.431
0.7288	-0.44	0.7300	-0.44	0.7313	-0.439	0.7326	-0.448	0.7339	-0.447
0.7351	-0.453	0.7364	-0.45	0.7377	-0.454	0.7389	-0.454	0.7403	-0.456
0.7417	-0.463	0.7430	-0.465	0.7444	-0.467	0.7458	-0.465	0.7473	-0.471
0.7487	-0.473	0.7501	-0.474	0.7515	-0.473	0.7530	-0.473	0.7544	-0.476
0.7558	-0.481	0.7573	-0.477	0.7587	-0.476	0.7601	-0.482	0.7616	-0.479
0.7630	-0.481	0.7644	-0.482	0.7659	-0.479	0.7673	-0.479	0.7687	-0.477
0.7702	-0.476	1.5975	-0.393	1.5988	-0.389	1.6001	-0.383	1.6015	-0.373
1.6028	-0.364	1.6041	-0.356	1.6055	-0.343	1.6068	-0.338	1.6082	-0.331
1.6095	-0.324	1.6108	-0.316	1.6122	-0.313	1.6135	-0.31	1.6148	-0.305
1.6162	-0.3	1.6175	-0.294	1.6189	-0.295	1.6202	-0.286	1.6219	-0.282
1.6236	-0.274	1.6253	-0.275	1.6269	-0.268	1.6286	-0.269	1.6303	-0.267
1.6320	-0.266	1.6337	-0.266	1.6354	-0.27	1.6371	-0.272	1.6404	-0.281
1.6419	-0.287	1.6433	-0.29	1.6448	-0.297	1.6462	-0.304	1.6477	-0.314
1.6492	-0.316	1.6506	-0.329	1.6521	-0.331	1.6535	-0.341	1.6549	-0.347
1.6563	-0.355	1.6577	-0.366	1.6592	-0.369	1.6606	-0.374	1.6620	-0.385
1.6634	-0.39	1.6651	-0.401	1.6667	-0.405	1.6684	-0.409	1.6698	-0.419
1.6713	-0.428	1.6728	-0.439	1.6743	-0.448	1.6758	-0.449	1.6773	-0.453
1.6789	-0.455	1.6811	-0.455	1.6834	-0.458	1.6853	-0.46	1.6873	-0.466
1.6890	-0.464	1.6908	-0.469	1.6925	-0.473	1.6942	-0.479	1.6959	-0.48
1.6976	-0.486	1.6993	-0.486	1.7010	-0.49	1.7028	-0.49	1.7046	-0.494
1.7064	-0.496	1.7081	-0.488	1.7100	-0.501	1.7116	-0.505	1.7132	-0.506
1.7148	-0.511	1.7164	-0.512	1.7180	-0.511	1.7197	-0.514	1.7213	-0.512
1.7229	-0.511	1.7245	-0.515	1.7261	-0.513	1.7277	-0.517	1.7294	-0.516
1.7310	-0.515	1.7326	-0.516	1.7342	-0.513	1.7358	-0.51	1.7374	-0.51
1.7391	-0.508	1.7407	-0.5	1.7423	-0.497	1.7439	-0.497	1.7455	-0.495
1.7471	-0.493	1.7488	-0.49	1.7504	-0.482	1.7520	-0.482	1.7536	-0.479
1.7553	-0.475	1.7569	-0.465	1.7585	-0.463	1.7601	-0.46	1.7617	-0.45
1.7633	-0.445	1.7650	-0.439	2.6199	-0.081	2.6232	-0.129	2.6264	-0.175
2.6280	-0.198	2.6296	-0.218	2.6312	-0.237	2.6329	-0.257	2.6345	-0.276
2.6365	-0.3	2.6382	-0.315	2.6398	-0.328	2.6414	-0.339	2.6430	-0.354
2.6446	-0.361	2.6462	-0.372	2.6479	-0.378	2.6495	-0.382	2.6527	-0.392
2.6543	-0.395	2.6559	-0.399	2.6576	-0.402	2.6592	-0.405	2.6608	-0.413
2.6623	-0.414	2.6639	-0.415	2.6654	-0.422	2.6668	-0.428	2.6682	-0.429
2.6696	-0.437	2.6710	-0.439	2.6724	-0.443	2.6737	-0.45	2.6750	-0.451
2.6763	-0.454	2.6776	-0.458	2.6789	-0.46	2.6803	-0.464	2.6816	-0.463
2.6829	-0.469	2.6842	-0.466	2.6855	-0.466	2.6868	-0.472	2.6882	-0.474
2.6895	-0.475	2.6908	-0.477	2.6921	-0.476	2.6934	-0.476	2.6947	-0.473
2.6961	-0.473	2.6974	-0.479	2.6987	-0.472	2.7000	-0.476	2.7013	-0.479
2.7026	-0.475	2.7040	-0.477	2.7053	-0.473	2.7066	-0.47	2.7078	-0.469
2.7090	-0.467	2.7103	-0.469	2.7115	-0.471	2.7127	-0.469	2.7139	-0.466
2.7151	-0.466	2.7164	-0.466	2.7176	-0.464	2.7188	-0.461	2.7200	-0.461
2.7213	-0.46	2.7225	-0.454	2.7237	-0.447	2.7249	-0.455	2.7262	-0.446
2.7274	-0.446	2.7286	-0.445	2.7298	-0.444	2.7310	-0.441	2.7323	-0.436
2.7335	-0.43	2.7347	-0.435	2.7359	-0.434	2.7372	-0.431	2.7384	-0.427
2.7396	-0.425	2.7408	-0.42	2.7421	-0.422	2.7433	-0.421	2.7445	-0.418

**Table A.1** — *Continued.*

HJD +2454770	$\Delta(m)$								
2.7457	-0.422	2.7469	-0.421	2.7482	-0.42	2.7496	-0.415	2.7509	-0.408
2.7523	-0.414	2.7537	-0.408	2.7551	-0.41	2.7568	-0.402	2.7587	-0.396
2.7607	-0.384	3.6054	-0.394	3.6065	-0.389	3.6129	-0.422	3.6140	-0.42
3.6152	-0.428	3.6163	-0.429	3.6175	-0.43	3.6186	-0.431	3.6198	-0.436
3.6209	-0.438	3.6221	-0.434	3.6232	-0.437	3.6244	-0.439	3.6255	-0.44
3.6267	-0.443	3.6279	-0.437	3.6290	-0.444	3.6302	-0.446	3.6313	-0.448
3.6325	-0.451	3.6336	-0.451	3.6348	-0.454	3.6359	-0.455	3.6371	-0.46
3.6382	-0.458	3.6394	-0.466	3.6405	-0.465	3.6417	-0.47	3.6429	-0.468
3.6440	-0.47	3.6452	-0.47	3.6463	-0.473	3.6475	-0.472	3.6486	-0.479
3.6497	-0.48	3.6508	-0.482	3.6519	-0.483	3.6530	-0.485	3.6541	-0.487
3.6552	-0.486	3.6563	-0.485	3.6574	-0.49	3.6585	-0.491	3.6596	-0.491
3.6607	-0.493	3.6619	-0.49	3.6630	-0.494	3.6641	-0.493	3.6652	-0.495
3.6663	-0.494	3.6674	-0.493	3.6685	-0.495	3.6696	-0.496	3.6707	-0.495
3.6718	-0.496	3.6729	-0.495	3.6740	-0.498	3.6751	-0.495	3.6762	-0.493
3.6773	-0.497	3.6785	-0.492	3.6796	-0.494	3.6807	-0.492	3.6818	-0.487
3.6829	-0.487	3.6840	-0.486	3.6851	-0.482	3.6862	-0.48	3.6873	-0.476
3.6884	-0.479	3.6895	-0.475	3.6906	-0.473	3.6917	-0.467	3.6928	-0.471
3.6940	-0.467	3.6951	-0.466	3.6962	-0.46	3.6973	-0.46	3.6984	-0.455
3.6995	-0.45	3.7006	-0.445	3.7017	-0.444	3.7028	-0.444	3.7039	-0.439
3.7050	-0.437	3.7061	-0.432	3.7073	-0.428	3.7086	-0.42	3.7098	-0.42
3.7111	-0.416	3.7123	-0.41	3.7136	-0.405	3.7149	-0.407	3.7161	-0.399
3.7174	-0.396	3.7188	-0.392	3.7201	-0.386	3.7217	-0.383	3.7233	-0.37
3.7249	-0.361	3.7266	-0.348	3.7282	-0.341	3.7298	-0.323	3.7314	-0.304
3.7330	-0.288	3.7346	-0.268	3.7363	-0.247	3.7379	-0.227	3.7395	-0.199
3.7411	-0.181	3.7428	-0.151	3.7451	-0.113	3.7476	-0.073	3.7526	0.003
3.7551	0.042	3.7576	0.076	3.7600	0.093	4.5924	-0.396	4.5937	-0.396
4.5949	-0.402	4.5962	-0.407	4.5975	-0.408	4.5987	-0.415	4.6000	-0.415
4.6013	-0.421	4.6026	-0.421	4.6038	-0.424	4.6051	-0.428	4.6064	-0.433
4.6076	-0.434	4.6089	-0.438	4.6102	-0.438	4.6114	-0.441	4.6127	-0.443
4.6140	-0.447	4.6153	-0.45	4.6165	-0.453	4.6178	-0.455	4.6189	-0.456
4.6201	-0.459	4.6212	-0.459	4.6223	-0.459	4.6234	-0.46	4.6246	-0.462
4.6257	-0.463	4.6268	-0.462	4.6280	-0.464	4.6291	-0.465	4.6302	-0.468
4.6314	-0.47	4.6325	-0.466	4.6337	-0.464	4.6348	-0.467	4.6360	-0.466
4.6371	-0.469	4.6383	-0.468	4.6394	-0.469	4.6406	-0.475	4.6417	-0.483
4.6429	-0.482	4.6440	-0.479	4.6452	-0.476	4.6464	-0.476	4.6475	-0.472
4.6487	-0.471	4.6498	-0.468	4.6510	-0.466	4.6521	-0.463	4.6533	-0.46
4.6545	-0.458	4.6557	-0.455	4.6570	-0.451	4.6582	-0.452	4.6595	-0.452
4.6607	-0.45	4.6619	-0.448	4.6633	-0.443	4.6647	-0.442	4.6660	-0.439
4.6674	-0.439	4.6688	-0.432	4.6702	-0.43	4.6716	-0.425	4.6730	-0.419
4.6743	-0.418	4.6757	-0.415	4.6771	-0.415	4.6785	-0.41	4.6799	-0.409
4.6813	-0.409	4.6827	-0.407	4.6842	-0.403	4.6856	-0.405	4.6871	-0.402
4.6886	-0.402	4.6901	-0.401	4.6916	-0.399	4.6931	-0.395	4.6946	-0.391
4.6961	-0.388	4.6976	-0.388	4.6992	-0.381	4.7007	-0.372	4.7022	-0.368
4.7037	-0.362	4.7052	-0.353	4.7067	-0.346	4.7082	-0.337	4.7097	-0.333
4.7112	-0.33	4.7127	-0.32	4.7142	-0.319	4.7157	-0.314	4.7172	-0.307
4.7187	-0.301	4.7202	-0.294	4.7217	-0.294	4.7232	-0.285	4.7247	-0.278
4.7262	-0.278	4.7278	-0.271	4.7293	-0.268	4.7309	-0.269	4.7325	-0.267
4.7341	-0.27	4.7358	-0.264	4.7376	-0.26	4.7394	-0.267	4.7411	-0.267
4.7429	-0.271	4.7446	-0.274	4.7464	-0.284	4.7482	-0.289	4.7500	-0.298
4.7519	-0.306	4.7537	-0.313	4.7554	-0.316	5.5976	-0.493	5.5989	-0.492
5.6001	-0.497	5.6014	-0.495	5.6027	-0.494	5.6039	-0.495	5.6051	-0.495
5.6062	-0.495	5.6074	-0.496	5.6085	-0.495	5.6097	-0.495	5.6109	-0.495
5.6120	-0.494	5.6132	-0.492	5.6143	-0.49	5.6155	-0.494	5.6166	-0.49
5.6178	-0.486	5.6189	-0.483	5.6201	-0.482	5.6212	-0.482	5.6224	-0.478
5.6235	-0.471	5.6247	-0.469	5.6259	-0.472	5.6270	-0.47	5.6282	-0.466
5.6293	-0.467	5.6305	-0.466	5.6316	-0.463	5.6328	-0.463	5.6339	-0.458
5.6351	-0.457	5.6362	-0.453	5.6374	-0.45	5.6385	-0.447	5.6397	-0.444
5.6408	-0.447	5.6420	-0.437	5.6432	-0.437	5.6443	-0.435	5.6455	-0.434

**Table A.1** — *Continued.*

HJD +2454770	$\Delta(m)$								
5.6466	-0.423	5.6478	-0.418	5.6489	-0.419	5.6501	-0.409	5.6512	-0.409
5.6524	-0.408	5.6535	-0.401	5.6547	-0.396	5.6558	-0.393	5.6570	-0.388
5.6581	-0.389	5.6593	-0.39	5.6605	-0.382	5.6616	-0.38	5.6628	-0.374
5.6639	-0.371	5.6651	-0.362	5.6662	-0.353	5.6674	-0.348	5.6685	-0.336
5.6697	-0.33	5.6708	-0.311	5.6720	-0.296	5.6731	-0.282	5.6743	-0.27
5.6755	-0.255	5.6766	-0.241	5.6778	-0.226	5.6789	-0.209	5.6801	-0.193
5.6812	-0.172	5.6824	-0.159	5.6837	-0.136	5.6851	-0.114	5.6865	-0.095
5.6879	-0.075	5.6893	-0.053	5.6906	-0.032	5.6920	-0.01	5.6934	0.013
5.6948	0.03	5.6962	0.051	5.6976	0.068	5.6990	0.085	5.7003	0.095
5.7017	0.104	5.7031	0.115	5.7045	0.118	5.7059	0.117	5.7073	0.121
5.7086	0.113	5.7100	0.104	5.7115	0.098	5.7131	0.085	5.7147	0.063
5.7163	0.045	5.7179	0.021	5.7196	-0.005	5.7214	-0.031	5.7231	-0.062
5.7249	-0.093	5.7266	-0.119	5.7284	-0.146	5.7301	-0.171	5.7318	-0.193
5.7336	-0.218	5.7354	-0.238	5.7371	-0.257	5.7388	-0.281	5.7406	-0.296
5.7423	-0.313	5.7441	-0.327	5.7458	-0.342	5.7475	-0.349	5.7493	-0.357
5.7510	-0.37								

**Table A.2** *R* Band Observations of 1RXS J201607.0+251645

HJD +2454770	$\Delta(m)$								
0.6420	-0.253	0.6431	-0.236	0.6441	-0.22	0.6452	-0.207	0.6462	-0.187
0.6472	-0.172	0.6483	-0.157	0.6496	-0.14	0.6509	-0.124	0.6522	-0.11
0.6535	-0.093	0.6548	-0.078	0.6561	-0.066	0.6575	-0.052	0.6588	-0.046
0.6601	-0.04	0.6614	-0.034	0.6627	-0.03	0.6641	-0.036	0.6654	-0.039
0.6667	-0.042	0.6680	-0.049	0.6693	-0.058	0.6706	-0.069	0.6719	-0.086
0.6731	-0.099	0.6744	-0.119	0.6757	-0.135	0.6769	-0.15	0.6782	-0.173
0.6793	-0.182	0.6804	-0.205	0.6815	-0.213	0.6826	-0.235	0.6837	-0.252
0.6847	-0.265	0.6858	-0.283	0.6869	-0.3	0.6880	-0.315	0.6890	-0.326
0.6900	-0.341	0.6911	-0.354	0.6921	-0.365	0.6931	-0.384	0.6942	-0.391
0.6952	-0.4	0.6963	-0.41	0.6973	-0.427	0.6983	-0.433	0.6994	-0.437
0.7004	-0.45	0.7015	-0.456	0.7025	-0.463	0.7035	-0.472	0.7046	-0.475
0.7056	-0.48	0.7066	-0.484	0.7077	-0.487	0.7088	-0.49	0.7100	-0.498
0.7111	-0.497	0.7123	-0.498	0.7135	-0.501	0.7147	-0.511	0.7160	-0.511
0.7172	-0.514	0.7184	-0.522	0.7196	-0.522	0.7208	-0.528	0.7220	-0.526
0.7232	-0.532	0.7244	-0.537	0.7255	-0.538	0.7268	-0.544	0.7282	-0.542
0.7295	-0.549	0.7308	-0.553	0.7320	-0.551	0.7333	-0.554	0.7346	-0.558
0.7359	-0.556	0.7371	-0.562	0.7384	-0.565	0.7397	-0.566	0.7410	-0.564
0.7424	-0.569	0.7438	-0.573	0.7452	-0.575	0.7466	-0.576	0.7480	-0.578
0.7495	-0.582	0.7509	-0.579	0.7523	-0.582	0.7538	-0.585	0.7552	-0.588
0.7566	-0.585	0.7580	-0.585	0.7595	-0.587	0.7609	-0.588	0.7623	-0.59
0.7638	-0.584	0.7652	-0.589	0.7666	-0.591	0.7681	-0.583	0.7695	-0.585
1.5982	-0.498	1.5995	-0.49	1.6009	-0.484	1.6022	-0.476	1.6035	-0.47
1.6049	-0.455	1.6062	-0.447	1.6075	-0.438	1.6089	-0.432	1.6102	-0.428
1.6116	-0.418	1.6129	-0.413	1.6142	-0.407	1.6156	-0.403	1.6169	-0.394
1.6182	-0.391	1.6196	-0.382	1.6212	-0.378	1.6228	-0.374	1.6245	-0.367
1.6262	-0.364	1.6279	-0.356	1.6296	-0.355	1.6313	-0.357	1.6330	-0.356
1.6346	-0.355	1.6363	-0.359	1.6380	-0.365	1.6397	-0.37	1.6413	-0.368
1.6427	-0.379	1.6442	-0.384	1.6456	-0.393	1.6471	-0.397	1.6485	-0.401
1.6500	-0.413	1.6515	-0.42	1.6529	-0.423	1.6544	-0.432	1.6558	-0.44
1.6572	-0.45	1.6586	-0.459	1.6600	-0.466	1.6614	-0.474	1.6628	-0.476
1.6642	-0.489	1.6659	-0.498	1.6676	-0.504	1.6692	-0.513	1.6707	-0.521
1.6722	-0.528	1.6737	-0.539	1.6752	-0.54	1.6767	-0.543	1.6782	-0.548
1.6804	-0.546	1.6826	-0.552	1.6845	-0.555	1.6865	-0.557	1.6882	-0.557
1.6900	-0.56	1.6917	-0.564	1.6934	-0.572	1.6952	-0.571	1.6969	-0.575
1.6985	-0.578	1.7002	-0.582	1.7019	-0.589	1.7037	-0.587	1.7055	-0.592

**Table A.2 — *Continued.***

HJD +2454770	$\Delta(m)$								
1.7073	-0.591	1.7090	-0.594	1.7109	-0.597	1.7125	-0.598	1.7141	-0.603
1.7158	-0.601	1.7174	-0.603	1.7190	-0.605	1.7206	-0.61	1.7222	-0.609
1.7238	-0.605	1.7255	-0.605	1.7271	-0.609	1.7287	-0.608	1.7303	-0.608
1.7319	-0.605	1.7336	-0.603	1.7352	-0.605	1.7368	-0.6	1.7384	-0.602
1.7400	-0.6	1.7416	-0.598	1.7433	-0.599	1.7449	-0.599	1.7465	-0.595
1.7481	-0.59	1.7497	-0.587	1.7514	-0.585	1.7530	-0.583	1.7546	-0.579
1.7562	-0.576	1.7578	-0.566	1.7594	-0.56	1.7611	-0.558	1.7627	-0.55
1.7643	-0.544	1.7659	-0.546	2.6157	-0.149	2.6175	-0.178	2.6193	-0.2
2.6209	-0.226	2.6225	-0.247	2.6241	-0.271	2.6257	-0.291	2.6273	-0.315
2.6290	-0.338	2.6306	-0.355	2.6322	-0.375	2.6338	-0.392	2.6375	-0.431
2.6391	-0.446	2.6407	-0.456	2.6424	-0.469	2.6440	-0.479	2.6456	-0.491
2.6472	-0.499	2.6488	-0.503	2.6504	-0.504	2.6521	-0.51	2.6537	-0.509
2.6553	-0.52	2.6569	-0.521	2.6585	-0.522	2.6601	-0.525	2.6617	-0.53
2.6632	-0.532	2.6648	-0.538	2.6663	-0.543	2.6677	-0.547	2.6691	-0.551
2.6704	-0.559	2.6718	-0.563	2.6731	-0.564	2.6745	-0.566	2.6758	-0.572
2.6771	-0.575	2.6784	-0.575	2.6797	-0.577	2.6810	-0.582	2.6824	-0.578
2.6837	-0.578	2.6850	-0.581	2.6863	-0.584	2.6876	-0.582	2.6889	-0.585
2.6903	-0.59	2.6916	-0.587	2.6929	-0.591	2.6942	-0.594	2.6955	-0.589
2.6968	-0.59	2.6981	-0.583	2.6995	-0.591	2.7008	-0.591	2.7021	-0.59
2.7034	-0.587	2.7047	-0.588	2.7060	-0.588	2.7073	-0.589	2.7085	-0.585
2.7098	-0.581	2.7110	-0.586	2.7122	-0.588	2.7134	-0.585	2.7147	-0.584
2.7159	-0.581	2.7171	-0.575	2.7183	-0.575	2.7195	-0.583	2.7208	-0.575
2.7220	-0.573	2.7232	-0.571	2.7244	-0.57	2.7257	-0.568	2.7269	-0.569
2.7281	-0.568	2.7293	-0.561	2.7306	-0.561	2.7318	-0.556	2.7330	-0.556
2.7342	-0.553	2.7354	-0.555	2.7367	-0.548	2.7379	-0.548	2.7403	-0.538
2.7416	-0.542	2.7428	-0.54	2.7440	-0.534	2.7452	-0.54	2.7465	-0.539
2.7477	-0.529	2.7489	-0.534	2.7503	-0.532	2.7517	-0.523	2.7531	-0.527
2.7545	-0.524	2.7559	-0.519	2.7579	-0.514	2.7598	-0.509	2.7617	-0.504
3.6060	-0.491	3.6071	-0.503	3.6135	-0.531	3.6146	-0.535	3.6158	-0.54
3.6169	-0.538	3.6181	-0.538	3.6192	-0.543	3.6204	-0.544	3.6215	-0.543
3.6227	-0.546	3.6239	-0.55	3.6250	-0.55	3.6262	-0.549	3.6273	-0.552
3.6285	-0.554	3.6296	-0.554	3.6308	-0.556	3.6319	-0.561	3.6331	-0.56
3.6342	-0.564	3.6354	-0.561	3.6365	-0.567	3.6377	-0.568	3.6389	-0.571
3.6400	-0.576	3.6412	-0.576	3.6423	-0.574	3.6435	-0.579	3.6446	-0.579
3.6458	-0.582	3.6469	-0.584	3.6481	-0.586	3.6492	-0.585	3.6503	-0.586
3.6514	-0.588	3.6525	-0.589	3.6536	-0.588	3.6547	-0.588	3.6558	-0.59
3.6569	-0.591	3.6580	-0.593	3.6591	-0.595	3.6603	-0.594	3.6614	-0.595
3.6625	-0.596	3.6636	-0.595	3.6647	-0.599	3.6658	-0.598	3.6669	-0.598
3.6680	-0.6	3.6691	-0.601	3.6702	-0.601	3.6713	-0.597	3.6724	-0.599
3.6735	-0.599	3.6746	-0.598	3.6757	-0.6	3.6769	-0.595	3.6780	-0.592
3.6791	-0.594	3.6802	-0.589	3.6813	-0.588	3.6824	-0.589	3.6835	-0.586
3.6846	-0.584	3.6857	-0.581	3.6868	-0.582	3.6879	-0.576	3.6890	-0.575
3.6901	-0.575	3.6912	-0.569	3.6923	-0.564	3.6935	-0.565	3.6946	-0.565
3.6957	-0.561	3.6968	-0.559	3.6979	-0.553	3.6990	-0.554	3.7001	-0.55
3.7012	-0.543	3.7023	-0.543	3.7034	-0.543	3.7045	-0.537	3.7056	-0.536
3.7069	-0.529	3.7081	-0.532	3.7093	-0.525	3.7105	-0.518	3.7118	-0.515
3.7131	-0.51	3.7143	-0.514	3.7156	-0.505	3.7169	-0.499	3.7181	-0.498
3.7195	-0.497	3.7210	-0.489	3.7226	-0.483	3.7242	-0.478	3.7258	-0.467
3.7275	-0.453	3.7291	-0.441	3.7307	-0.425	3.7323	-0.413	3.7339	-0.399
3.7355	-0.376	3.7372	-0.356	3.7388	-0.334	3.7404	-0.309	3.7421	-0.287
3.7466	-0.222	3.7491	-0.186	3.7516	-0.152	3.7541	-0.119	3.7566	-0.083
3.7591	-0.058	4.5931	-0.509	4.5944	-0.511	4.5957	-0.519	4.5969	-0.525
4.5982	-0.53	4.5995	-0.528	4.6007	-0.532	4.6020	-0.534	4.6033	-0.536
4.6046	-0.541	4.6058	-0.542	4.6071	-0.546	4.6084	-0.548	4.6096	-0.553
4.6109	-0.555	4.6122	-0.56	4.6134	-0.563	4.6147	-0.564	4.6160	-0.568
4.6172	-0.57	4.6184	-0.574	4.6196	-0.572	4.6207	-0.579	4.6218	-0.574
4.6230	-0.578	4.6241	-0.577	4.6252	-0.58	4.6264	-0.578	4.6275	-0.578
4.6286	-0.579	4.6298	-0.58	4.6309	-0.583	4.6320	-0.582	4.6332	-0.584

**Table A.2** — *Continued.*

HJD +2454770	$\Delta(m)$								
4.6343	-0.582	4.6355	-0.583	4.6366	-0.585	4.6378	-0.585	4.6389	-0.582
4.6401	-0.588	4.6412	-0.589	4.6424	-0.596	4.6436	-0.595	4.6447	-0.594
4.6459	-0.592	4.6470	-0.589	4.6482	-0.587	4.6493	-0.585	4.6505	-0.583
4.6516	-0.579	4.6528	-0.58	4.6540	-0.575	4.6552	-0.575	4.6564	-0.569
4.6577	-0.57	4.6589	-0.57	4.6602	-0.569	4.6614	-0.566	4.6627	-0.563
4.6641	-0.56	4.6655	-0.562	4.6669	-0.557	4.6683	-0.555	4.6696	-0.549
4.6710	-0.542	4.6724	-0.537	4.6738	-0.54	4.6752	-0.535	4.6766	-0.534
4.6780	-0.53	4.6793	-0.53	4.6807	-0.524	4.6821	-0.527	4.6836	-0.524
4.6850	-0.522	4.6865	-0.52	4.6879	-0.515	4.6894	-0.517	4.6909	-0.516
4.6924	-0.511	4.6939	-0.506	4.6954	-0.504	4.6970	-0.499	4.6985	-0.496
4.7000	-0.49	4.7015	-0.489	4.7030	-0.483	4.7045	-0.471	4.7060	-0.462
4.7075	-0.454	4.7090	-0.448	4.7105	-0.438	4.7120	-0.432	4.7135	-0.427
4.7150	-0.423	4.7165	-0.417	4.7180	-0.411	4.7195	-0.408	4.7240	-0.384
4.7255	-0.386	4.7271	-0.375	4.7286	-0.373	4.7302	-0.364	4.7318	-0.36
4.7334	-0.357	4.7351	-0.348	4.7369	-0.355	4.7386	-0.353	4.7421	-0.361
4.7439	-0.366	4.7475	-0.381	4.7493	-0.389	4.7511	-0.393	4.7547	-0.418
4.7564	-0.417	5.5982	-0.605	5.5995	-0.608	5.6008	-0.608	5.6021	-0.602
5.6033	-0.605	5.6046	-0.611	5.6057	-0.604	5.6069	-0.602	5.6081	-0.602
5.6092	-0.605	5.6104	-0.603	5.6115	-0.607	5.6127	-0.604	5.6138	-0.604
5.6150	-0.605	5.6161	-0.594	5.6173	-0.597	5.6184	-0.594	5.6196	-0.594
5.6207	-0.591	5.6219	-0.597	5.6230	-0.589	5.6242	-0.586	5.6254	-0.583
5.6265	-0.583	5.6277	-0.58	5.6288	-0.58	5.6300	-0.576	5.6311	-0.574
5.6323	-0.576	5.6334	-0.569	5.6346	-0.564	5.6357	-0.562	5.6369	-0.56
5.6380	-0.557	5.6392	-0.555	5.6404	-0.558	5.6415	-0.547	5.6427	-0.545
5.6438	-0.538	5.6450	-0.541	5.6461	-0.535	5.6473	-0.53	5.6484	-0.53
5.6496	-0.528	5.6507	-0.521	5.6519	-0.523	5.6530	-0.515	5.6542	-0.514
5.6553	-0.512	5.6565	-0.514	5.6577	-0.511	5.6588	-0.51	5.6600	-0.512
5.6611	-0.501	5.6623	-0.499	5.6634	-0.491	5.6646	-0.483	5.6669	-0.472
5.6680	-0.455	5.6692	-0.452	5.6703	-0.444	5.6715	-0.428	5.6727	-0.415
5.6738	-0.397	5.6750	-0.386	5.6761	-0.373	5.6773	-0.363	5.6784	-0.338
5.6796	-0.324	5.6807	-0.303	5.6819	-0.297	5.6831	-0.276	5.6845	-0.258
5.6859	-0.24	5.6873	-0.216	5.6886	-0.194	5.6900	-0.177	5.6914	-0.153
5.6928	-0.137	5.6956	-0.105	5.6970	-0.079	5.6983	-0.066	5.6997	-0.059
5.7011	-0.049	5.7025	-0.044	5.7039	-0.037	5.7053	-0.026	5.7080	-0.036
5.7094	-0.041	5.7109	-0.051	5.7124	-0.067	5.7140	-0.075	5.7157	-0.094
5.7173	-0.111	5.7189	-0.138	5.7206	-0.158	5.7224	-0.188	5.7242	-0.21
5.7276	-0.269	5.7294	-0.288	5.7311	-0.313	5.7329	-0.332	5.7346	-0.357
5.7381	-0.399	5.7398	-0.421	5.7416	-0.429	5.7433	-0.449	5.7451	-0.456
5.7468	-0.467	5.7503	-0.492						